Diffusion-limited electrochemical D-fructose sensor based on direct electron transfer-type bioelectrocatalysis by a variant of D-fructose dehydrogenase at a porous gold microelectrode

Yohei Suzuki, Kenji Kano, Osamu Shirai, Yuki Kitazumi*

Division of Applied Life Sciences, Graduate School of Agriculture, Kyoto University,

Sakyo, Kyoto 606-8502, Japan

* Corresponding author
Tel: +81 75 753 6393; fax: +81 75 753 6456.
E-mail address: kitazumi.yuki.7u@kyoto-u.ac.jp

ABSTRACT

An electrochemical D-fructose sensor was fabricated by immobilizing a variant of D-fructose dehydrogenase on a porous gold microelectrode. The enzyme-modified electrode bioelectrocatalytically oxidizes D-fructose via direct electron transfer. The catalytic current reaches a steady-state limiting value at 0.05 V vs. Ag|AgCl (sat. KCl). The temperature dependence of the sensor suggests that its response is limited by the diffusion of D-fructose. Therefore, the sensor requires no calibration. The sensitivity of the sensor, $(2.0 \pm 0.2) \times 10^2$ μA cm^{-2} mM^{-1}, is reproducible. The upper limit of detection is ~2.0 mM and the kinetics of the bioelectrocatalytic reaction is determined the limitation. The fabricated sensors were applied in the determination of D-fructose in commercial beverages as well as honey, and compared favorably with a more commonly used photometric method.

Keywords: D-fructose dehydrogenase, amperometric biosensor, direct electron transfer, microelectrode, porous gold

1. Introduction

D-Fructose in the blood has been related to obesity and various conditions such as cardiorenal and fatty liver diseases [1–3]. Therefore, the quantitative analysis of D-fructose in bodily fluids and consumer products is essential for the diagnosis of metabolic disorders as well as for quality assurance for fruits and beverages [4]. Quantitative analyses of D-fructose are typically based on titration [5], chromatography [6], spectrophotometry [7], and fluorimetry [8]. However, such methods are time-consuming because they are usually carried out in batch formats and require pretreatments such as filtration and the addition of reagents.

Brief, rapid analyses of D-fructose are possible with electrochemical biosensors that operate under mild conditions based on bioelectrocatalysis, which couples an electrode reaction and a redox enzymatic reaction [9–11]. The selectivity of the enzymatic reaction minimizes the pretreatment of the sample to be evaluated. Direct electron transfer (DET)-type bioelectrocatalysis, in which enzymes exchange electrons directly with the electrode, is suitable for the construction of cheap and stable electrochemical devices [12–20].

Electrochemical biosensors for D-fructose have been realized via DET-type bioelectrocatalysis by D-fructose dehydrogenase (FDH; EC 1.1.99.11) from *Gluconobacter japonicus* NBRC 3260 [21–25]. This enzyme catalyzes the oxidation of D-fructose to 5-keto-D-fructose in the presence of electron acceptors. Native FDH is a heterotrimeric membrane-bound protein with a molecular mass of ca. 140 kDa that is comprised of subunits I (67 kDa), II (51 kDa), and III (20 kDa). Subunit I has a covalently bound flavin adenine dinucleotide (FAD) and subunit II has three heme *c* moieties (heme 1*c*, heme 2*c*, heme 3*c*, from the N- to the C-terminus) [26,27]. In DET-type bioelectrocatalysis by FDH, the electron is transferred from the reduced FAD through heme 3*c*, heme 2*c*, and then to the electrode; heme 1*c* is not thought to be involved in the electron transfer pathway [28,29].

Interference in biosensing from some reductants in the sample, such as L-ascorbate, can be eliminated by operating at rather negative potentials. To promote D-fructose oxidation under such a condition, a variant of FDH (M450QΔ1*c*FDH) was constructed by the protein engineering approach [30]. In this variant, 143 amino acid residues involving heme 1*c* were removed, and M450 as the sixth axial ligand of heme 2*c* was replaced with glutamine. The DET-type bioelectrocatalytic activity of M450QΔ1*c*FDH (~0 V vs. Ag|AgCl (sat. KCl)) is higher than that of recombinant (native)

FDH (rFDH). The replacement of the axial ligand of heme 2*c* shifts its redox potential negatively. Furthermore, the removal of the region including heme 1*c* reduces the size of the enzyme. Therefore, the surface concentration of the variant on the electrode can be increased. Based on these characteristics, M450QΔ1*c*FDH is a more suitable enzyme for D-fructose sensing than rFDH.

Steady-state characteristics are important in amperometric biosensors. Because the steady-state response of microdisk electrodes is independent of time due to spherical diffusion, microdisk electrodes are suitable for use in electrochemical sensing. Additionally, electrochemical sensors with microelectrodes are useful for pathological examination because smaller quantities of samples are required. The steady-state limiting current of a microdisk electrode is formulated as follows [31]:

$$I = 4nFcDr, \quad (1)$$

where I is the current, n is the number of electrons, F is the Faraday constant, c is the bulk concentration of the substrate, D is the diffusion coefficient of the substrate, and r is the electrode radius. According to Eq. 1, the steady-state sensitivity of microdisk electrode-type sensors depends on r and D alone. Thus, substrate quantification is possible without calibration. Moreover, the response of the microdisk electrode increases with decreases in r. Therefore, microdisk electrodes have excellent characteristics for electrochemical sensors.

To apply the characteristics of microelectrodes to amperometric biosensors, it is necessary to realize bioelectrocatalysis controlled by the mass transfer of the substrate to the electrode surface. Therefore, the enzymatic reaction must be significantly faster than the mass transfer of the substrate [32–34]. DET-type bioelectrocatalysis at a porous electrode would be a reasonable solution, because abundant FDH can be effectively adsorbed on the electrode and DET-type catalytic activity can be effectively utilized by the curvature effects of the porous structure; the population of the enzyme orientations suitable for DET-type bioelectrocatalysis increases in mesoporous structures with radius close to that of enzymes [35–39]. Several porous electrodes have been developed as scaffolds to obtain DET-type bioelectrocatalysis by FDH, including ketjen black [40], porous carbon [41], carbon nanotubes [42,43], and colloidal Au [44]. Because it is difficult to construct a microelectrode from powdered materials, we focused on the anodization of Au microelectrodes to fabricate porous Au microelectrodes [38,45–48]. In this work, a diffusion-limited electrochemical D-fructose sensor was developed by immobilizing M450QΔ1*c*FDH on a porous Au microelectrode. The characteristics of the constructed biosensor were investigated, and the sensor was used to quantify D-fructose in commercial beverages and honey.

2. Experimental

2.1. Materials and reagents

2-Mercaptoethanol was purchased from Nacalai Tesque Co., Ltd. (Japan). Other chemicals were obtained from Wako Pure Chemical Industries, Ltd. (Japan). All chemicals employed in this work were of analytical grade and were used without any purification.

M450QΔ1*c*FDH was expressed and purified as described in previous work and stored as a solution of pH 4.5 McIlvaine buffer containing 0.1% Triton® X-100 and 1 mM 2-mercaptoethanol as the stabilizer (specific activity: 2×10^{10} U mol^{-1}, protein concentration: 10 μM) [27,49]. Commercial beverages (a fruit juice (Dole® apple juice) and carbonated drink (C.C. Lemon, Suntory Foods Limited, Japan)) and Chinese honey were purchased in a local market. Epoxy resins (Torr Seal and Scotch-Weld™ EPX™ DP 100 clear) were purchased from Agilent Technologies, Inc. (USA) and 3M Japan Limited (Japan), respectively. A conductive adhesive (Dotite D-362) was obtained from Fujikura Kasei Co., Ltd. (Japan). Au wire (99.95%, diameter: 0.1 mm) and Cu wire (99.9%, diameter: 1.0 mm) were purchased from The Nilaco Corporation. (Japan).

2.2. Fabrication of enzyme-modified microelectrodes

Au microelectrodes were fabricated from a gold wire, a copper wire, and epoxy resins based on a previous report [47]. The fabricated Au microelectrodes were cut crosswise using an abrasive cutter (RC-120, As One Co., Ltd., Japan) to expose the Au wire, and polished using a grinding wheel. Then, the microelectrode was washed in deionized water for 30 s at room temperature using an ultrasonic disperser (UT-305S, Sharp Co., Ltd., Japan). A porous microelectrode was prepared by oxidation in 0.1 M (M = mol dm^{-3}) phosphate buffer (pH 7) containing 0.8 M KCl at 1.29 V vs. Ag|AgCl (sat. KCl) for 120 s [38]. To modify the electrode potential to the desired adsorption potential of FDH (<0.6 V [50]), the fabricated porous electrode was reduced in McIlvaine buffer (pH 4.5) by applying a potential scan from 0.6 to 0 V vs. Ag|AgCl (sat. KCl) at a scan rate (v) of 20 mV s^{-1}; then, the electrode was left for 1 h in the buffer solution for stabilization. The radius of the fabricated porous electrode was measured using an optical microscope (VHX-100 digital microscope, Keyence Co., Ltd., Japan). The recorded current was normalized by the projected area of the electrode.

After casting an aliquot of FDH or M450QΔ1*c*FDH solution (15 μL) onto the fabricated microporous electrode, the electrode was left for 10 min at 4 °C. Finally, the

enzyme-modified electrode was gently washed with McIlvaine buffer (pH 4.5) to remove excess enzyme.

2.3. Electrochemical measurements

Electrochemical measurements were carried out using an electrochemical analyzer (HZ-3000, Hokuto Denko Co., Ltd., Japan). A handmade Ag|AgCl (sat. KCl) electrode and a platinum wire were used as the reference and counter electrodes, respectively. All potentials are referred to the reference electrode in this study. The measurements were performed in deaired McIlvaine buffer (pH 4.5, 14 mL). The temperature of the cell was controlled using a water-jacketed cell holder at 25 °C. All experiments were carried out in a Faraday cage to reduce electrical disturbance.

2.4. Photometric determination of D-fructose.

The determination of D-fructose in commercial beverage samples was performed spectrophotometrically with a 5 μL aliquot of FDH solution, potassium ferricyanide (as an electron acceptor), and ferric sulfate-Dupanol reagent, as described in the literature [26]. A calibration curve was prepared using a standard solution of D-fructose (R^2 = 0.999). The juice, carbonated drink, and honey were diluted with McIlvaine buffer (pH 4.5) at dilution ratios of 1:1000 for the beverages and 1:10000 for the honey.

3. Results and discussion

3.1. DET-type bioelectrocatalysis of M450QΔ1*c*FDH at the microelectrode

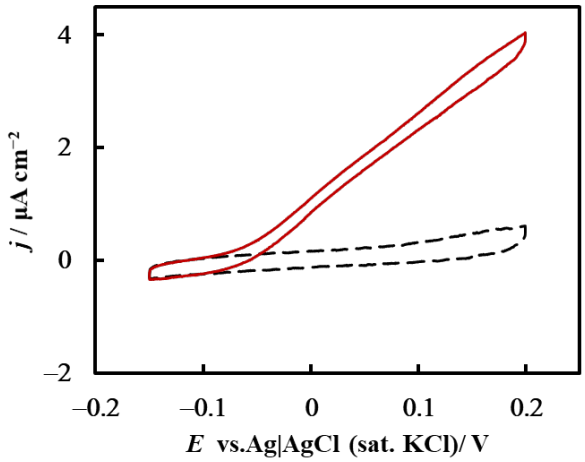

Fig. 1. Cyclic voltammograms for the oxidation of D-fructose at M450QΔ1*c*FDH-modified planar Au microelectrodes with r = 52 μm at c = 1.0 mM and v = 2 mV s^{-1}. The solid and broken lines represent voltammograms recorded in the presence and absence of D-fructose, respectively.

Figure 1 shows cyclic voltammograms recorded at the M450QΔ1*c*FDH-modified planar Au microelectrode. The solid and broken lines represent voltammograms recorded in the presence and absence of 1 mM D-fructose, respectively. The catalytic oxidation of D-fructose is observed to occur at potentials more positive than −0.1 V. However, the oxidation current increased with an increase in the electrode potential. Above an applied potential of 0.5 V, the catalytic currents decrease due to the formation of a Au oxide layer (data not shown) [29,50,51]. The potential-dependence of the bioelectrocatalytic current is known as a residual slope [13]. The residual slope on the voltammogram demonstrates that the oxidation current is controlled by the bioelectrocatalysis of M450QΔ1*c*FDH. Since the activity of the enzyme was insufficient to realize a substrate-transfer-controlled current at the planar Au microelectrode, a porous Au microelectrode was employed to increase the adsorbed amount of M450QΔ1*c*FDH and improve the bioelectrocatalysis of D-fructose oxidation.

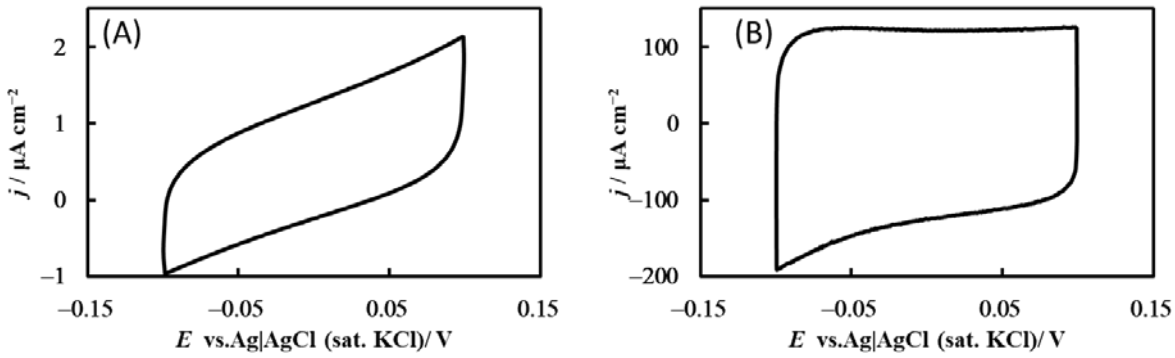

Fig. 2. Cyclic voltammograms for the charging currents of a microdisk electrode with r = 52 μm recorded at v = 10 mV s^{-1} (A) before and (B) after anodization.

The anodization of a Au microdisk electrode effectively increases its surface area. Figure 2 shows the cyclic voltammograms of the charging currents of Au microdisk electrodes around 0 V (A) before and (B) after anodization and stabilization. The electrode surface turns black after anodization. Assuming that the double-layer capacitance of the electrode at 0 V remained unchanged through anodization, the electrochemically effective surface area of the electrode was evaluated to increase 170-fold by the anodization from an increase in the charging current. The increase in the charging current and color change of the electrode surface demonstrate that anodization results in the formation of porous structures on the electrode surface. According to previous works [38], the nanoporous structure is constructed with cylindrical components and has pores of 20 to 200 nm.

Figure 3 shows cyclic voltammograms recorded at the M450QΔ1*c*FDH-modified porous Au microdisk electrode. The solid and broken lines represent voltammograms recorded in the presence and absence of 1 mM D-fructose, respectively. The catalytic oxidation current reaches the potential-independent limiting value at voltages more positive than 0.05 V. The porous structure increases the catalytic current by ~300 times at –0.05 V. The increased ratio of the catalytic current was larger than that expected from the increase in the electrochemically active surface area by the anodization. The phenomena seem to be attributed to the curvature effect at the porous electrode surface on the DET-type bioelectrocatalysis of M450QΔ1*c*FDH [38,46]. The concave surface of the nanoporous structure will improve the probability of the effectively oriented enzyme for the DET-type bioelectrocatalysis. The potential-independent bioelectrocatalytic current at the porous Au microdisk electrode demonstrates that the rate-determining step is changed from the enzymatic reaction to the mass transfer reaction of the substrate. Therefore, the enzymatic reaction rate is not uniform at the surface of the

electrode. The enzymes which are advantageous for the supply of the substrate will work preferentially at the electrode surface.

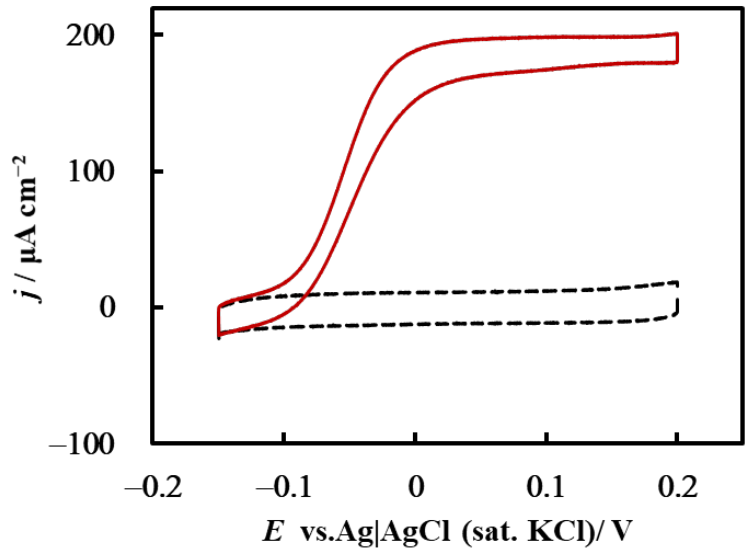

Fig. 3. Cyclic voltammograms of the oxidation of D-fructose at an M450QΔ1*c*FDH-modified porous Au microelectrode with r = 52 μm at c = 1.0 mM and v = 2 mV s^{-1}. The solid and broken lines represent voltammograms recorded in the presence and absence of D-fructose, respectively.

3.2. Response of the M450QΔ1*c*FDH-modified electrode

Figure 4A shows the chronoamperogram recorded by the M450QΔ1*c*FDH-modified electrode at 0.05 V with successive additions of D-fructose. The oxidation current increases with increasing D-fructose concentration, reaching steady-state values 30 s after the addition of the substrate. The steady-state currents were stable for at least 2 min.

Figures 4B and 4C show the calibration curve for D-fructose using the constructed biosensor. When the concentration of D-fructose is higher than 100 mM, the catalytic current density no longer depends on the substrate concentration (Fig. 4B). Additionally, the catalytic current became poor in reproduciblity in this concentration range (data not shown). Above 100 mM, the enzymatic reaction controls the oxidation current. When the concentration of D-fructose is less than 2.0 mM, the current density

linearly increases with an increase in the substrate concentration (Fig. 4C). In this concentration region, the response of the sensor is highly reproducible. To discuss the stability of the sensor quantitatively, the coefficient of variation (CV = standard deviation (σ)/ mean (μ)) of the response was estimated from the data obtained from three sensors (Fig. 4D). Clearly, the values of CV are small at concentrations lower than 1.0 mM. Such high reproducibility of the sensor also supports the conclusion that the catalytic current is controlled by substrate diffusion from the bulk of the solution to the electrode surface.

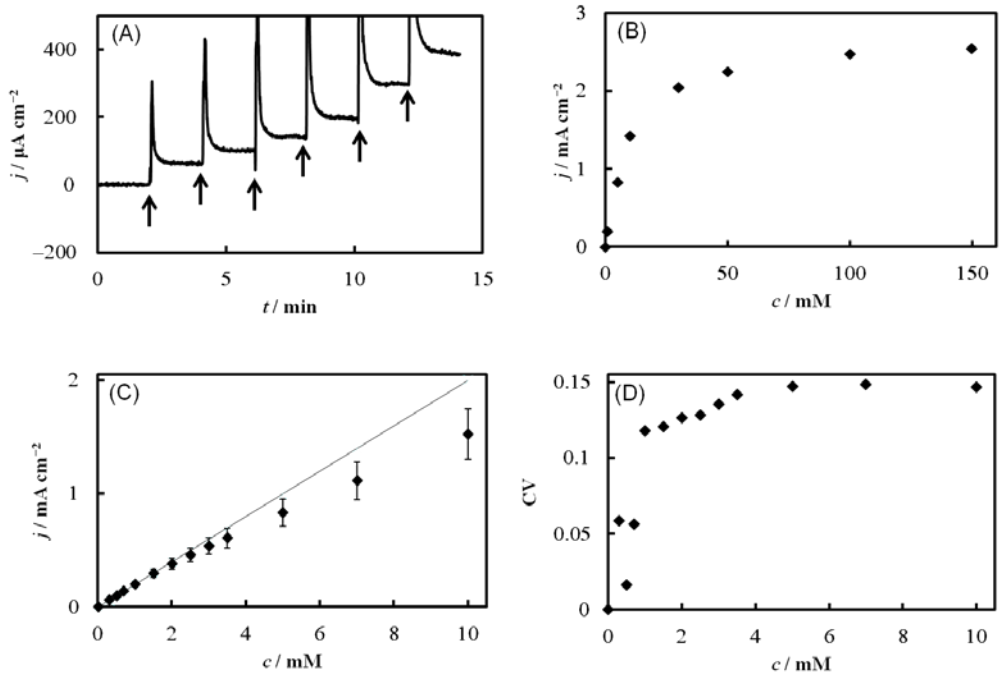

Fig. 4. (A) Chronoamperogram obtained from the fabricated sensor with r = 53 μm at a potential of 0.05 V. The substrate solution was added and the solution was stirred at the times indicated by the arrows. The bulk concentrations of the substrate at each arrow are 0.3, 0.5, 0.7, 1.0, 1.5, and 2.0 mM, from left to right. (B) Concentration dependence of the steady-state current of the constructed D-fructose biosensor. (C) Magnified view of the linear region of the calibration curve. Error bars show the 90% confidence level (n = 3). The solid line is the theoretical response under the diffusion-controlled conditions at the sensor estimated from Eq. (1) with r = 50 μm. (D) Coefficient of variation (CV = σ/μ) at each concentration.

3.3. Rate-determining bioelectrocatalytic step for the sensor

Figure 5A shows calibration curves based on chronoamperograms recorded with the M450QΔ1*c*FDH-modified electrode at 25 °C (diamonds) and 37 °C (squares) for different concentrations of D-fructose. The data confirm that the current density increases ~1.3-fold when the temperature changes from 25 to 37 °C. The diffusion coefficient (*D*) of a substrate increases with a rise in temperature, and its temperature dependence is described as follows:

$$D = D_0 \ \exp(-\frac{Q}{RT}) \qquad (2)$$

where D_0 is the frequency factor, Q is the activation energy, R is the gas constant, and T is the absolute temperature. Since the reported value of Q for D-fructose in aqueous solution is 15.64 kJ mol^{-1} [52], the ratio of the diffusion coefficients at 25 and 37 °C can be calculated as 1.28. This ratio agrees with the temperature dependence of the current density of the sensor, described above.

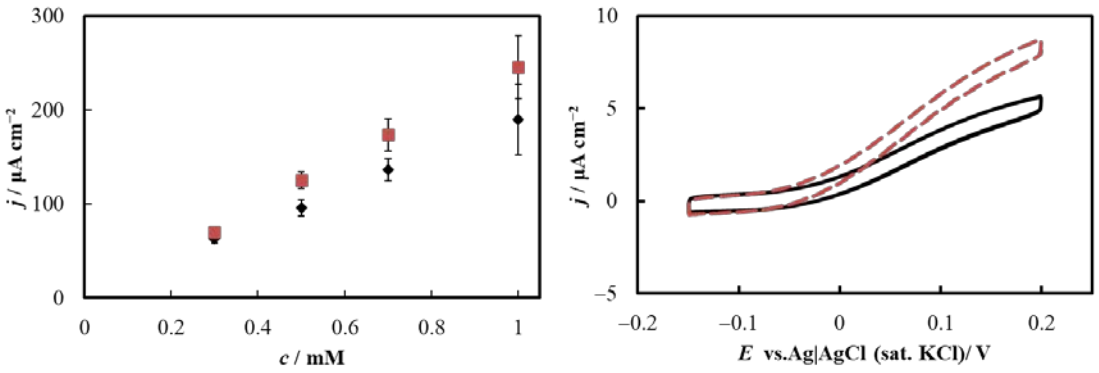

Fig. 5. (A) Calibration curves recorded at 0.05 V for sensors with r = 50 μm at 25 °C (diamonds) and 37 °C (squares). Error bars show the 90% confidence level (n = 3). (B) Cyclic voltammograms of D-fructose oxidation by M450QΔ1*c*FDH-modified electrode recorded at 25 °C (solid line) and 37 °C (broken line), c = 100 mM, r = 51 μm, and v = 2 mV s^{-1}.

On the other hand, the enzymatic reaction is also accelerated by an increase in temperature. Figure 5B shows the voltammograms recorded by the M450QΔ1*c*FDH-modified electrode at 25 and 37 °C, when c = 100 mM. The limiting current density at 0.05 V increases ~1.8 times with a rise in temperature. As judged from Fig. 4B, the current is controlled by the enzymatic reaction under these conditions. If the enzymatic reaction is the rate-determining step of the bioelectrocatalysis in the sensor, the expected current ratio at 25 and 37 °C would be ~1.8.

These results show that the origin of the sensitivity's temperature dependence when the concentration is lower than 1.0 mM is assigned to not the change in the kinetics of the enzymatic reaction but the change in the diffusion coefficient of D-fructose. The actual diffusion coefficient estimated from Eq. (1) and the slope of the calibration curve is calculated as $(4.1 \pm 0.4) \times 10^{-10}$ m^2 s^{-1} at 25 °C, which is slightly smaller than the literature value (6.89×10^{-10} m^2 s^{-1}, 2 mM, 25 °C) [52]. The discrepancy is probably due to the difference between the test solution and the measurement method. The solid line in Fig. 4C represents the theoretical response of the sensor with a sensitivity of (200 ± 20) μA cm^{-2} mM^{-1} estimated from Eq. (1). The experimentally recorded response agrees with the theoretical response, supporting the conclusion that the current in the linear region is controlled by the diffusion of D-fructose.

The adsorbed amount of M450QΔ1*c*FDH will be proportional to the enzymatic reaction controlled current. If the adsorbed amount of the enzyme satisfies that the catalytic current at c = 100 mM is greater than 2 mA cm^{-2}, the response of the sensor at c = 1 mM is independent in the adsorbed amount of the enzyme (Fig. S1). This insensitivity of the sensor agrees that the current is controlled by the diffusion of the substrate when the sufficient amounts of enzyme adsorbed at the electrode surface.

3.4. Selectivity and stability

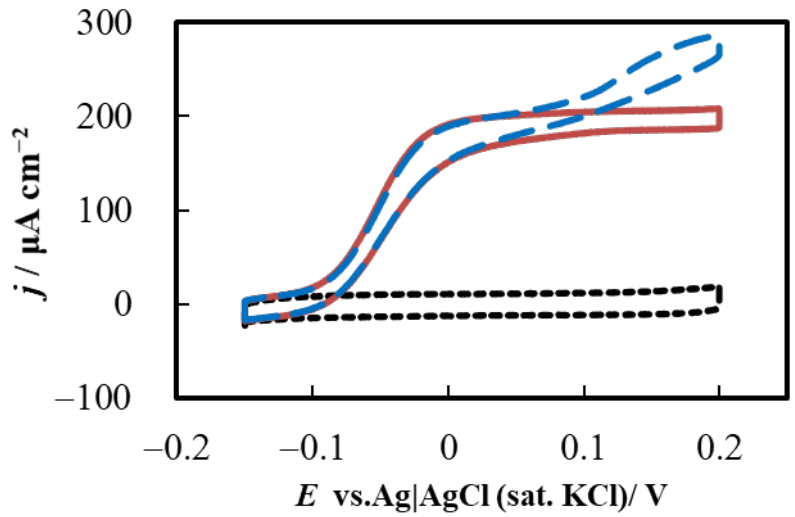

Fig. 6. Effect of L-ascorbate on the constructed D-fructose biosensor with r = 54 μm. The solid and broken lines represent voltammograms recorded in the absence and presence of

1 mM L-ascorbate in a buffer solution containing 1 mM D-fructose at v = 2 mV s^{-1}. The dotted line shows the background voltammogram.

The selectivity of the constructed D-fructose biosensor for coexisting substances was examined. Figure 6 shows cyclic voltammograms recorded by the M450QΔ1*c*FDH-modified electrode in buffer solution containing 1 mM D-fructose with (solid line) and without (broken line) 1 mM L-ascorbate. The direct oxidation current of L-ascorbate at the biosensor occurs with a half-wave potential of ~0.17 V. Assuming the half-wave potential is equal to the formal potential of L-ascorbate, the oxidation current at 0.05 V is ~1/10000 of its limiting current. Therefore, it can be concluded that the effect of the oxidation of L-ascorbate was practically negligible on the response of this biosensor working at 0.05 V. This result suggests that the sensor is applicable to the analysis of D-fructose in fruit juice containing massive amounts of L-ascorbate without pretreatment.

Oxygen is one of the major interfering oxidative substances in electrochemical sensors. Additionally, it has been reported that the oxygen reduction activity of a porous Au electrode is higher than that of a planar Au electrode [38]. However, the direct reduction current of oxygen in an aerated solution at the 450QΔ1*c*FDH-modified porous Au microelectrode is negligibly smaller than the oxidation current of D-fructose at 0.05 V (Fig. S2). Unfortunately, the response of the sensor is affected by hydrogen peroxide above 300 μM at 0.05 V (Fig. S3). The presence of neither 100 mM D-glucose nor 100 mM sucrose has an effect on the oxidation current of D-fructose at the sensor (Fig. S4). Therefore, the substrate selectivity of FDH is maintained even when the artificial mutation is used. The sensor's sensitivity in the presence of various interferents is listed in Table 1. The sensitivity of this sensor is stable, unless the viscosity of the sample remained unchanged.

Table 1. Effects of interferents on sensitivity

Substance	Sensitivity* /mA cm^{-2} mM^{-1}
1 mM L-ascorbate	0.19 ± 0.01
0.26 mM oxygen	0.19 ± 0.01
0.1 mM hydrogen peroxide	0.20 ± 0.01
100 mM D-glucose	0.19 ± 0.01
100 mM sucrose	0.19 ± 0.01

*confidence level: 90%, n = 3

The stability of the fabricated biosensor was evaluated based on its response to 1.0 mM D-fructose every 2 days. The sensor was stored at 4 °C in pH 4.5 McIlvaine buffer containing 0.1% Triton® X-100 and 1 mM 2-mercaptoethanol during lifetime evaluation. The catalytic current density for the oxidation of 1.0 mM D-fructose is independent of the storage time for up to 6 days (Fig. S5). After 8 days, the current decreases by 10%. Therefore, the biosensor requires no calibration for D-fructose detection for at least 6 days. The stability of the sensor can be improved by increasing the amount of adsorbed enzyme.

Table 2. Comparison of the characteristics of various amperometric fructose sensors.

Electrode	Electrolyte	Working potential / V vs. Ag/AgCl	Sensitivity ($\mu A\ cm^{-2}\ mM^{-1}$)	Reference
FDH/ferrocene-CPE	0.1 *M* phosphate buffer (pH 7.2)	0.5	50	[22]
FDH/TRGO	McIlvaine buffer (pH 4.5)	0.4	14.5	[23]
FDH/PG	McIlvaine buffer (pH 5.5)	0.15	3.7	[24]
FDH/4-APh/PG	Acetate buffer (pH 4.5)	0.20	175	[25]
M450QΔ1*c*FDH/ PG	McIlvaine buffer (pH 4.5)	0.05	200 ± 20	This work

CPE: carbon paste electrode
TRGO: thermally reduced graphene oxide
PG: porous gold
4-APh: 4-aminothiophenol

The characteristics of the sensor in this work are compared with those of the previously reported fructose biosensors. Table 2 summarizes the working conditions and sensitivities of the FDH based fructose biosensors. The fructose biosensor constructed in this work has a high sensitivity because of its mass transfer process-controlled response. Therefore, the agitation of the solution seriously affects the current (Fig. S1). Additionally, the working potential of the sensor is more negative than those for the other sensors due

to the adoption of M450QΔ1*c*FDH. The negative working potential of the present sensor provides high selectivity and enables the adaption of the calibration curve method to the real sample analysis.

3.5. Detection of D-fructose in commercial beverages

The fabricated biosensor was used to determine the content of D-fructose in commercial beverage and honey samples at 25 °C. The standard photometric method, which is widely employed for D-fructose analysis, was used for data comparison. Table 3 shows the quantified amounts of D-fructose in the three samples from Eq. 1. The biosensor-determined values agree with those quantified photometrically (confidence level of 90%). Therefore, the constructed biosensor can be used in the analysis of real samples without any pretreatment other than dilution.

Table 3. Quantified D-fructose contents in commercial beverages*

	Constructed biosensor	Photometric method
Fruit juice (mM)	320 ± 20	310 ± 30
Carbonated drink (mM)	220 ± 30	260 ± 20
Honey (mol kg^{-1})	2.3 ± 0.1	2.6 ± 0.2

*confidence level: 90%, $n = 3$

4. Conclusion

A diffusion-limited D-fructose biosensor was constructed from an M450QΔ1*c*FDH-immobilized porous Au microelectrode with $r = 50$ μm. The sensitivity of this sensor ($(2.0 \pm 0.2) \times 10^2$ μA cm^{-2} mM^{-1}) depended only on the temperature. Therefore, the sensor enabled rapid detection without calibration under the constant temperature. The upper limit of detection was ~2.0 mM. Owing to the more negative potential of M450QΔ1*c*FDH, the sensor can work at the negative potential of 50 mV vs. Ag|AgCl (sat. KCl), which the effect of the oxidation of L-ascorbate was practically negligible.

5. Acknowledgements

We would like to thank Editage (www.editage.com) for English language editing.

References

[1] R.J. Johnson, M.S. Segal, Y. Sautin, T. Nakagawa, D.I. Feig, D.H. Kang, M.S. Gersch, S. Benner, L.G. Sánchez-Lozada, Potential role of sugar (fructose) in the epidemic of hypertension, obesity and the metabolic syndrome, diabetes, kidney disease, and cardiovascular disease1-3, Am. J. Clin. Nutr. 86 (2007) 899–906. https://doi.org/10.1093/ajcn/86.4.899.

[2] X. Ouyang, P. Cirillo, Y. Sautin, S. McCall, J.L. Bruchette, A.M. Diehl, R.J. Johnson, M.F. Abdelmalek, Fructose consumption as a risk factor for non-alcoholic fatty liver disease, J. Hepatol. 48 (2008) 993–999. https://doi.org/10.1016/j.jhep.2008.02.011.

[3] L. Tappy, K.A. Lê, C. Tran, N. Paquot, Fructose and metabolic diseases: New findings, new questions, Nutrition. 26 (2010) 1044–1049. https://doi.org/10.1016/j.nut.2010.02.014.

[4] R. Antiochia, G. Vinci, L. Gorton, Rapid and direct determination of fructose in food: A new osmium-polymer mediated biosensor, Food Chem. 140 (2013) 742–747. https://doi.org/10.1016/j.foodchem.2012.11.023.

[5] G.P. Meade, J.C.P. Chen, Cane sugar handbook., John Wiley & Sons., New York., 1977.

[6] J.M. Langemeier, D.E. Rogers, Rapid method for sugar analysis of doughs and baked products, Cereal Chem. 72 (1995) 349–351.

[7] Z. Dische, E. Borenfreund, A new spectrophotometric method for the detection and determination of keto sugars and trioses, J. Biol. Chem. 192 (1951) 583–587.

[8] G. Pina Luis, M. Granda, R. Badía, M.E. Díaz-García, Selective fluorescent chemosensor for fructose, Analyst. 123 (1998) 155–158. https://doi.org/10.1039/a703778c.

[9] I. Willner, E. Katz, B. Willner, Electrical Contact of Redox Enzyme Layers Associated with Electrodes: Routes to Amperometric Biosensors, Electroanalysis. 9 (1997) 965–977. https://doi.org/10.1002/elan.1140091302.

[10] M. Stumpp, C. Lupo, D. Schlettwein, Preparation and Characterization of Electrodeposited ZnO on Microstructured Electrode Arrays, J. Electrochem. Soc. 159 (2012) D717–D723. https://doi.org/10.1149/2.041212jes.

[11] T. Gan, Z. Shi, J. Sun, Y. Liu, Simple and novel electrochemical sensor for the determination of tetracycline based on iron/zinc cations-exchanged montmorillonite catalyst, Talanta. 121 (2014) 187–193. https://doi.org/10.1016/j.talanta.2014.01.002.

[12] S. V. Hexter, T.F. Esterle, F.A. Armstrong, A unified model for surface electrocatalysis based on observations with enzymes, Phys. Chem. Chem. Phys. 16 (2014) 11822–11833. https://doi.org/10.1039/c3cp55230f.

[13] C. Léger, P. Bertrand, Direct electrochemistry of redox enzymes as a tool for mechanistic studies, Chem. Rev. 108 (2008) 2379–2438. https://doi.org/10.1021/cr0680742.

[14] M.J. Moehlenbrock, S.D. Minteer, Extended lifetime biofuel cells, Chem. Soc. Rev. 37 (2008) 1188–1196. https://doi.org/10.1039/b708013c.

[15] N. Mano, F. Mao, A. Heller, A miniature membrane-less biofuel cell operating at +0.60 V under physiological conditions, ChemBioChem. 5 (2004) 1703–1705. https://doi.org/10.1002/cbic.200400275.

[16] D. Leech, P. Kavanagh, W. Schuhmann, Enzymatic fuel cells: Recent progress, Electrochim. Acta. 84 (2012) 223–234. https://doi.org/10.1016/j.electacta.2012.02.087.

[17] S.C. Barton, J. Gallaway, P. Atanassov, Enzymatic biofuel cells for implantable and microscale devices, Chem. Rev. 104 (2004) 4867–4886. https://doi.org/10.1021/cr020719k.

[18] N. Mano, L. Edembe, Bilirubin oxidases in bioelectrochemistry: Features and recent findings, Biosens. Bioelectron. 50 (2013) 478–485. https://doi.org/10.1016/j.bios.2013.07.014.

[19] J.A. Cracknell, K.A. Vincent, F.A. Armstrong, Enzymes as working or inspirational electrocatalysts for fuel cells and electrolysis, Chem. Rev. 108 (2008) 2439–2461. https://doi.org/10.1021/cr0680639.

[20] L. Gorton, A. Lindgren, T. Larsson, F.D. Munteanu, T. Ruzgas, I. Gazaryan, Direct electron transfer between heme-containing enzymes and electrodes as basis for third generation biosensors, Anal. Chim. Acta. 400 (1999) 91–108. https://doi.org/10.1016/S0003-2670(99)00610-8.

[21] T. Ikeda, F. Matsushita, M. Senda, Amperometric fructose sensor based on direct bioelectrocatalysis, Biosens. Bioelectron. 6 (1991) 299–304. https://doi.org/10.1016/0956-5663(91)85015-O.

[22] M. Boujtita, N. El Murr, Ferrocene-Mediated Carbon Paste Electrode Modified with D-Fructose Dehydrogenase for Batch Mode Measurement of D-Fructose, Appl. Biochem. Biotechnol. 89 (2000) 55-69. https://doi.org/10.1385/ABAB:89:1:55.

[23] I. Šakinyte, J. Barkauskas, J. Gaidukevič, J. Razumiene, Thermally reduced graphene oxide: The study and use for reagentless amperometric d-fructose

biosensors, Talanta. 144 (2015) 1096-1103. https://doi.org/10.1016/j.talanta.2015.07.072.

[24] T. Siepenkoetter, U. Salaj-Kosla, E. Magner, The Immobilization of Fructose Dehydrogenase on Nanoporous Gold Electrodes for the Detection of Fructose, ChemElectroChem. 4 (2017) 905–912. https://doi.org/10.1002/celc.201600842.

[25] P. Bollella, Y. Hibino, K. Kano, L. Gorton, R. Antiochia, Highly sensitive membraneless fructose biosensor based on fructose dehydrogenase immobilized onto aryl thiol modified highly porous gold electrode: characterization and application in food samples, Anal. Chem. 90 (2018) 12131-12136. https://doi.org/10.1021/acs.analchem.8b03093.

[26] M. Ameyama, E. Shinagawa, K. Matsushita, O. Adachi, D-fructose dehydrogenase of Gluconobacter industrius: purification, characterization, and application to enzymatic microdetermination of D-fructose, J. Bacteriol. 145 (1981) 814–823. https://doi.org/10.1128/jb.145.2.814-823.1981.

[27] S. Kawai, M. Goda-Tsutsumi, T. Yakushi, K. Kano, K. Matsushita, Heterologous overexpression and characterization of a flavoprotein-cytochrome c complex fructose dehydrogenase of Gluconobacter japonicus NBRC3260, Appl. Environ. Microbiol. 79 (2013) 1654–1660. https://doi.org/10.1128/AEM.03152-12.

[28] S. Kawai, T. Yakushi, K. Matsushita, Y. Kitazumi, O. Shirai, K. Kano, The electron transfer pathway in direct electrochemical communication of fructose dehydrogenase with electrodes, Electrochem. Commun. 38 (2014) 28–31. https://doi.org/10.1016/j.elecom.2013.10.024.

[29] Y. Hibino, S. Kawai, Y. Kitazumi, O. Shirai, K. Kano, Mutation of heme c axial ligands in d-fructose dehydrogenase for investigation of electron transfer pathways and reduction of overpotential in direct electron transfer-type bioelectrocatalysis, Electrochem. Commun. 67 (2016) 43–46. https://doi.org/10.1016/j.elecom.2016.03.013.

[30] Y. Hibino, S. Kawai, Y. Kitazumi, O. Shirai, K. Kano, Protein-engineering improvement of direct electron transfer-type bioelectrocatalytic properties of D-fructose dehydrogenase, Electrochemistry. 87 (2019) 47–51. https://doi.org/10.5796/electrochemistry.18-00068.

[31] K. Aoki, Theory of ultramicroelectrodes, Electroanalysis, 5 (1993) 627–639. https://doi.org/10.1002/elan.1140050802.

[32] T. Noda, M. Wanibuchi, Y. Kitazumi, S. Tsujimura, S. Osamu, M. Yamamoto, K. Kano, Diffusion-controlled detection of glucose with microelectrodes in mediated

bioelectrocatalytic oxidation, Anal. Sci. 29 (2013) 279–281. https://doi.org/10.2116/analsci.29.279.

[33] Y. Matsui, K. Hamamoto, Y. Kitazumi, O. Shirai, K. Kano, Diffusion-controlled mediated electron transfer-type bioelectrocatalysis using microband electrodes as ultimate amperometric glucose sensors, Anal. Sci. 33 (2017) 845–851. https://doi.org/10.2116/analsci.33.845.

[34] T. Adachi, Y. Kaida, Y. Kitazumi, O. Shirai, K. Kano, Bioelectrocatalytic performance of D-fructose dehydrogenase, Bioelectrochemistry. 129 (2019) 1–9. https://doi.org/10.1016/j.bioelechem.2019.04.024.

[35] A. Walcarius, S.D. Minteer, J. Wang, Y. Lin, A. Merkoçi, Nanomaterials for bio-functionalized electrodes: Recent trends, J. Mater. Chem. B. 1 (2013) 4878–4908. https://doi.org/10.1039/c3tb20881h.

[36] A. De Poulpiquet, A. Ciaccafava, R. Gadiou, S. Gounel, M.T. Giudici-Orticoni, N. Mano, E. Lojou, Design of a H2/O2 biofuel cell based on thermostable enzymes, Electrochem. Commun. 42 (2014) 72–74. https://doi.org/10.1016/j.elecom.2014.02.012.

[37] K. Komori, T. Tatsuma, Y. Sakai, Direct Electron Transfer Kinetics of Peroxidase at Edge Plane Sites of Cup-Stacked Carbon Nanofibers and Their Comparison with Single-Walled Carbon Nanotubes, Langmuir. 32 (2016) 9163–9170. https://doi.org/10.1021/acs.langmuir.6b02407.

[38] M. Miyata, K. Kano, O. Shirai, Y. Kitazumi, Rapid fabrication of nanoporous gold as a suitable platform for the direct electron transfer-type bioelectrocatalysis of bilirubin oxidase, Electrochemistry, in printing.

[39] M. Wanibuchi, Y. Takahashi, Y. Kitazumi, O. Shirai, K. Kano, Significance of Nano-Structures of Carbon Materials for Direct-Electron-Transfer-type Bioelectrocatalysis of Bilirubin Oxidase, Electrochemistry, in printing. https://doi.org/10.5796/electrochemistry.20-64063.

[40] Y. Kamitaka, S. Tsujimura, K. Kano, High current density bioelectrolysis of D-fructose at fructose dehydrogenase-adsorbed and Ketjen black-modified electrodes without a mediator, Chem. Lett. 36 (2007) 218–219. https://doi.org/10.1246/cl.2007.218.

[41] S. Tsujimura, A. Nishina, Y. Kamitaka, K. Kano, Coulometric D-fructose biosensor based on direct electron transfer using D-fructose dehydrogenase, Anal. Chem. 81 (2009) 9383–9387. https://doi.org/10.1021/ac901771t.

[42] M. Tominaga, S. Nomura, I. Taniguchi, d-Fructose detection based on the direct heterogeneous electron transfer reaction of fructose dehydrogenase adsorbed onto

multi-walled carbon nanotubes synthesized on platinum electrode, Biosens. Bioelectron. 24 (2009) 1184–1188. https://doi.org/10.1016/j.bios.2008.07.002.

[43] J. Chen, D. Bamper, D.T. Glatzhofer, D.W. Schmidtke, Development of Fructose Dehydrogenase-Ferrocene Redox Polymer Films for Biofuel Cell Anodes, J. Electrochem. Soc. 162 (2015) F258–F264. https://doi.org/10.1149/2.0291503jes.

[44] S. Yabuki, F. Mizutani, D-Fructose Sensing Electrode Based on Electron Transfer of D-Fructose Dehydrogenase at Colloidal Gold-Enzyme Modified Electrode, Electroanalysis. 9 (1997) 23–25. https://doi.org/10.1002/elan.1140090107.

[45] K. Sakai, Y. Kitazumi, O. Shirai, K. Kano, Nanostructured porous electrodes by the anodization of gold for an application as scaffolds in direct-electron-transfer-type bioelectrocatalysis, Anal. Sci. 34 (2018) 1317–1322. https://doi.org/10.2116/analsci.18P302.

[46] Y. Takahashi, M. Wanibuchi, Y. Kitazumi, O. Shirai, K. Kano, Improved direct electron transfer-type bioelectrocatalysis of bilirubin oxidase using porous gold electrodes, J. Electroanal. Chem. 843 (2019) 47–53. https://doi.org/10.1016/j.jelechem.2019.05.007.

[47] M. Miyata, Y. Kitazumi, O. Shirai, K. Kataoka, K. Kano, Diffusion-limited biosensing of dissolved oxygen by direct electron transfer-type bioelectrocatalysis of multi-copper oxidases immobilized on porous gold microelectrodes, J. Electroanal. Chem. 860 (2020) 113895. https://doi.org/10.1016/j.jelechem.2020.113895.

[48] Y. Xia, W. Huang, J. Zheng, Z. Niu, Z. Li, Nonenzymatic amperometric response of glucose on a nanoporous gold film electrode fabricated by a rapid and simple electrochemical method, Biosens. Bioelectron. 26 (2011) 3555–3561. https://doi.org/10.1016/j.bios.2011.01.044.

[49] Y. Hibino, S. Kawai, Y. Kitazumi, O. Shirai, K. Kano, Construction of a protein-engineered variant of D-fructose dehydrogenase for direct electron transfer-type bioelectrocatalysis, Electrochem. Commun. 77 (2017) 112–115. https://doi.org/10.1016/j.elecom.2017.03.005.

[50] Y. Sugimoto, Y. Kitazumi, O. Shirai, M. Yamamoto, K. Kano, Role of 2-mercaptoethanol in direct electron transfer-type bioelectrocatalysis of fructose dehydrogenase at Au electrodes, Electrochim. Acta. 170 (2015) 242–247. https://doi.org/10.1016/j.electacta.2015.04.164.

[51] Y. Kaida, Y. Hibino, Y. Kitazumi, O. Shirai, K. Kano, Ultimate downsizing of D-fructose dehydrogenase for improving the performance of direct electron transfer-

type bioelectrocatalysis, Electrochem. Commun. 98 (2019) 101–105. https://doi.org/10.1016/j.elecom.2018.12.001.

[52] A.C.F. Ribeiro, O. Ortona, S.M.N. Simões, C.I.A.V. Santos, P.M.R.A. Prazeres, A.J.M. Valente, V.M.M. Lobo, H.D. Burrows, Binary mutual diffusion coefficients of aqueous solutions of sucrose, lactose, glucose, and fructose in the temperature range from (298.15 to 328.15) K, J. Chem. Eng. Data. 51 (2006) 1836–1840. https://doi.org/10.1021/je0602061.